Advances in Optoelectronic Technology and Industry Development – Jose & Ferreira (eds)

Electrically-modulated optoelectronics-based infrared source enabling ground surface precision deflectometry

Henry Quach
James C. Wyant College of Optical Sciences, University of Arizona, Tucson, AZ, USA

Logan R. Graves
James C. Wyant College of Optical Sciences, University of Arizona, Tucson, AZ, USA
Intuitive Optical Design Lab, Tucson, AZ, USA

Hyukmo Kang
James C. Wyant College of Optical Sciences, University of Arizona, Tucson, AZ, USA

Dae Wook Kim
James C. Wyant College of Optical Sciences, University of Arizona, Tucson, AZ, USA
Department of Astronomy, University of Arizona, Tucson, AZ, USA

ABSTRACT: We introduce the design of a scalable, modulated long-wave infrared source. The design makes use of a pseudo-blackbody heating element array, which radiates into a custom aluminum integrating cavity. The elements possess low thermal capacitance, enabling temporal modulation for improved signal isolation and dynamic background removal. To characterize performance, deflectometry measurements were made using both the new source design and a traditional tungsten ribbon source, which possess similar source irradiance and identical emission profile dimensions. Measurements from a ground glass flat and an aluminum blank demonstrated the new source produces a signal-to-noise ratio four times greater than that of the ribbon. Thermal imaging demonstrated improved source geometry and signal stability over time, and further, the new design measured a previously untestable hot aluminum flat (150 °C). The new design enables high-contrast thermal measurement of surfaces typically challenging to infrared deflectometry due to high surface roughness or intrinsic thermal noise generation.

Keywords optical metrology, deflectometry, infrared source, temporal modulation

1 INTRODUCTION

Freeform optics, or non-rotationally symmetric, highly custom-shaped optics, present the opportunity to improve the performance of an optical system. Under the assumption that an arbitrary surface can be fabricated, freeform optical designs may benefit from improved mechanical compactness, reduced assembly complexity, and better imaging performance (Fang et al., 2013). Across astronomical optics, medical imaging, defense, and consumer electronics, a new generation of optical instruments are on the horizon thanks to the flexibility conferred by these optics. However, as the popularity and diverseness off reeform optical surfaces grow, so do the metrology requirements.

Non-contact metrology off reeform optics is commonly performed by interferometry and deflectometry (Kim et al., 2016). Interferometry is a null metrology method, requiring a null optic to use as a reference against the unit under test (UUT). Particularly for freeform surfaces,

custom null optics are required. Diffractive elements called computer-generated holograms (CGH) are attractive null element options because they can null up to and including arbitrary surfaces with extreme or high-frequency features (Dubin et al., 2009). However, a CGH is typically designed for only one null configuration and may not always be a viable option for testing.

Alternatively, deflectometry is a non-null test method that has demonstrated comparable performance to interferometry over a range off reeform surfaces (Graves et al., 2019). In this method, an illumination source emits a known pattern, which specularly reflects off the UUT, and the reflected image of the source is captured by a camera. With precise knowledge of the setup's geometry, the local slopes of the UUT can be determined and integrated to generate a reconstructed surface map. Deflectometry carries the advantages of high testable slope dynamic range and measurement flexibility because it does not require a null reference. Of interest to optical fabrication, measurement of surface figure error during intermediary grinding phases may help prioritize local figure error correction so that a surface may more efficiently converge. Due to rapidly-changing surface profiles during grinding, CGHs are not practical, but deflectometry can become applicable if a camera and source of appropriate wavelength satisfy the specular reflectance condition (Oh et al., 2016; Lowman et al., 2018).

For optics in the grinding phase, which have a rough diffusing surface, a specular reflection can be achieved using long-wave infrared (LWIR) light, specifically, in the ~7-14 μm region. LWIR cameras are readily obtainable, but LWIR thermal source options are currently limited. One common design is implemented by applying a current to a thin tungsten ribbon, which induces joule heating and creates a rectangular, pseudo-blackbody emitting source (Su et al., 2011, 2013; Oh et al., 2016). By scanning this rectangular ribbon in orthogonal directions, a line scanning source is created, and slope information can be obtained to construct a full aperture surface sag map. While this source enables infrared deflectometry testing of rough surfaces at a precision scale, several inherent characteristics including low signal-to-noise ratio (SNR), limited modulation depth, and low temporal stability, limit the testing accuracy and range.

We have created a new source design which addresses these prior issues and extends the applicable range ofi nfrared deflectometry testing. The source is a Long-wave Infrared Time-Modulated Integrating cavity Source (LITMIS), which uses modular high efficiency and high stability resistive membrane pseudo-blackbody elements. A performance comparison was made against the traditional tungsten ribbon source, whose shape was identical to the exit slit of the box, using the same setup and LWIR camera. Results show promise in deflectometric testing of rough optics during their grinding phase and UUTs under thermal load.

2 TEMPORALLY MODULATED INFRARED SOURCE FOR DEFLECTOMETRY

2.1 Deflectometry overview

Deflectometry is a non-null technique that measures surface slopes of an optical surface, which are post-processed to reconstruct the surface. Dynamic range limitations are imposed by the source size, the camera field of view (FOV), and whether the UUT surface can reflect light emitted from the source. If a deflectometry setup can capture light reflected by the UUT, it can measure the local slopes of the UUT surface (Graves et al., 2019). Combined with precise system calibration data, slopes may be integrated in post-processing to reconstruct surface maps with accuracy comparable to that produced by interferometry (Martin et al., 2018).

In a typical deflectometry configuration, a high-resolution camera possessing a well-defined entrance pupil location, referred to as p(x,y,z), focuses onto the UUT surface. Camera pixels are mapped to the UUT surface, which is represented by discrete mirror pixels', referred to as u(x,y,z). Ideally, the source for a deflectometry setup, referred to as s(x,y,z), has high stability, repeatability, and signal power, which provide the test system with a high signal-to-noise ratio (SNR). At a single camera pixel that successfully captures light reflected from the UUT surface, the precise location on the source that illuminated the camera pixel is determined. Using the determined ray start location at the source, the end location at the camera, and the intercept location at the mirror pixel, the local slope at the mirror pixel can be calculated. This process is

extended to all camera pixels to measure the local slopes at all mirror pixels on the UUT in orthogonal directions, referred to as $S_X(x,y,z)$ and $S_Y(x,y,z)$, representing the x and y slopes respectively. These slope maps are typically integrated with a zonal integration method such as Southwell integration (Southwell, 1980) or a modal integration such as using a gradient Chebyshev polynomial set (Aftab et al., 2018), resulting in a reconstructed surface map. Figure 1 demonstrates a standard deflectometry setup and the model used for local slope calculation.

2.2 Infrared deflectometry and existing tungsten wire paradigm

Infrared deflectometry extends deflectometry to measuring diffuse rough optics, which are challenging to measure using traditional techniques. Because a wide range of materials and surfaces do not specularly reflect visible light, infrared deflectometry is an important metrology tool. This is particularly true during the grinding phase of mirror fabrication, where a rough grit is used to rapidly grind the UUT down to the final desired surface shape. During this period, the root-mean-square (RMS) surface roughness will typically drop from 100 µm to 1 µm as smaller grit sizes are used. For such rough surfaces, visible light is scattered and thus visible spectrum metrology tools are inapplicable; however, infrared deflectometry has been applied during this phase successfully for several mirror fabrication projects, including the Daniel K. Inouye Solar Telescope (DKIST) primary mirror (Oh et al., 2016).

Traditionally, a heated tungsten ribbon acts as the infrared source, serving as a pseudo-blackbody element. Coupled with a LWIR camera, which is sensitive in the 7-14µm range, this source allows for testing 1µm to ~25 µm RMS rough surfaces (Su et al., 2013; Kim et al., 2015, 2016; Oh et al., 2016). This test setup has been successfully used to measure a variety of rough, non-specularly reflecting surfaces and was able to achieve high accuracy surface reconstruction. It should be noted that other dynamic thermal pattern generators, including a scanning infrared laser and a resistor array, have successfully been used as sources for infrared deflectometry. However, a heated scanning ribbon still serves as the most common source for testing large diffuse optics (Höfer et al., 2016).

2.3 Compact, infrared pseudo-blackbody emitter

While a tungsten ribbon source can be engineered for higher signal power or larger size, its design is particularly vulnerable to thermal fatigue and suffers from several inherent limitations. Cyclically heated tungsten evaporates and degrades with use over time, leading to a potentially non-uniform emission profile across the surface. This is coupled with the nature

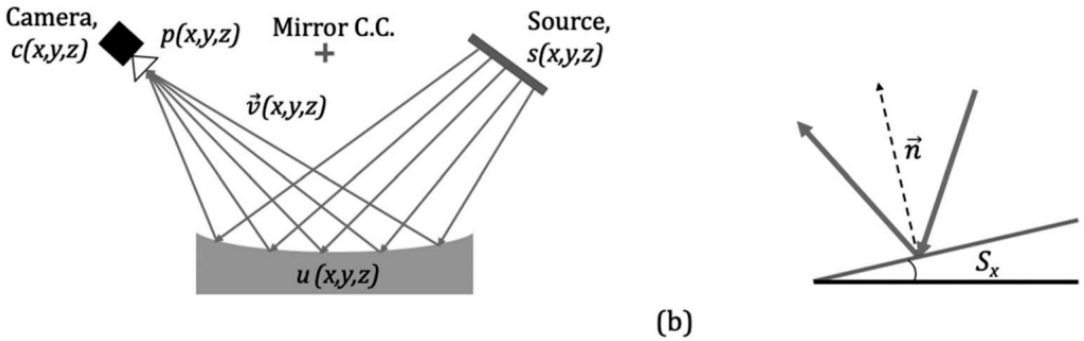

Figure 1. In a standard deflectometry system (a), light is emitted by a source, s(x,y,z). Some of the emitted light will deflect from the UUT surface, u(x,y,z), and be successfully captured by the camera, c(x,y,z), with an entrance pupil location, p(x,y,z). Represented by the vector $\vec{v}(x,y,z)$, a deflected light ray follows the law of reflection and is reflected by a local area on the UUT surface, whose normal vector is given by $\vec{n}$. Knowing the ray start, intercept, and end location, the local slope of the UUT, given by S_X, can be determined (b).

of a thin ribbon to possibly experience any of its lower bending modes during testing, further deviating the emission area from the theoretical ideal rectangular area. Additionally, driving higher input current through the ribbon only accelerates material degradation and also shifts the output spectrum away from desirable longer wavelengths. Finally, the heated tungsten ribbon invariably creates a temperature gradient in the surrounding air due to local convective boundary conditions. For larger ribbons and longer source operation time, growing pockets ofl ocally heated air may generate thermal noise that blurs the infrared source signal.

We propose an alternative source called a Long-wave Infrared Time-modulated Integrating cavity Source (LITMIS) to address these limitations. At the core of the LITMIS design is modular usage of EMIRS200 Series emitters, which are available commercially off-the-shelf from Axetris AG. The packaged emitters, henceforth referred to as'caps', are typically used in nondispersive infrared (NDIR) and photoacoustic gas spectroscopy and have a usable lifetime of 10,000 hours (Esfahani & Covington, 2017; Wilson et al., 2019). Although the emissive spectral distribution is centered at 4 µm at the operational temperature (550°C), radiant flux across the desired 7-12 µm band ofi nterest is also produced, as described by Planck's Law. Caps are fabricated by electroplating Platinum Black, a platinum powder, onto a thin membrane which floats on a silicon substrate (Hessler et al., 2004; Axetris AG, 2014, 2019). Similar to the tungsten ribbon, a cap is operated by driving an electric current through the target material to induce resistive heating and emit blackbody radiation. Two desirable source properties result from the cap material design and geometry:

High emissivity: when electroplated onto a substrate, Platinum Black forms dendritic structures on the scale of < 50 nm. The feature scale and high porosity of the structure result in high absorptivity and high emissivity ($\varepsilon > 0.9$) characteristics for the coated membrane, unlike that of smooth metallic surfaces. For example, the typical emissivity of tungsten is $\varepsilon < 0.1$ at 1000K (Verret & Ramanathan, 1978).

Low thermal capacitance: this property, also called thermal mass, refers to a body's ability to store thermal energy. Here, the combined resistive network of an exterior Platinum Black coating, Tantalum Oxide, and a SiN membrane is only several microns thick (Hessler et al., 2004), as compared to a typical ~30µm thick tungsten ribbon. Because the ultra-low mass is suspended in air by a silicon substrate, the thin emissive network can heat to and cool from its steady-state temperature in less than 1 second (Hessler et al., 2004).

Temporal modulation emerges as a viable operational mode of the new source. Testing reveals that a cap can achieve an 80% contrast ratio at 1 Hz, which enables in-situ background noise images to be taken during testing. Therefore, at a given image capture, a pair of 'signal' and 'background' shots can be successively captured for noise subtraction in post-processing.

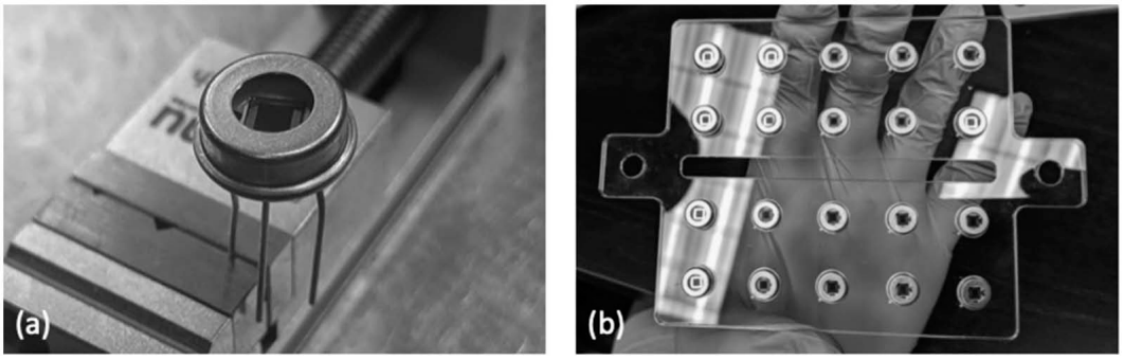

Figure 2. The Axetris EMIRS200 TO39 source features a resistive membrane that, when current is applied, acts as a pseudo-blackbody source (a). The emitters can be connected in series or in parallel, much likea group of resistors, to create a patterned source (b).

This option is not practical for the tungsten ribbon source because its relatively higher thermal mass evinces a slower thermal transient response. For any thermal source, noise will accumulate in the environment as it warms up and approaches its steady-state operational temperature.

2.4 Long-wave infrared time-modulated integrating cavity source

The Long-wave Infrared Time-modulated Integrating cavity Source (LITMIS) leverages the EMIRS200 elements as flexibly placed, highly time-responsive input nodes for radiative emission. Nodes radiate LWIR spectra into the integrating cavity, where the light is scattered and achieves a uniform, non-directional emission when exiting the rectangular output slit. Cavity length, interior wall roughness, and exit slit geometry are all optimized to minimize reflection losses. Furthermore, interior walls may be protected with high reflectivity coatings, like silver or gold, and the number ofi nput caps may be increased to scale power output.

For direct comparison with the ribbon source modality, an integrating cavity was designed and machined to match the geometrical and radiometric properties of an existing, functional tungsten rectangular ribbon source used for deflectometry (Su et al., 2011). These properties include source surface area and source radiance. The cavity was designed with 20 input 'cap' sources, operating at approximately 70% maximum power for safety and in order to achieve a 1 Hz flicker rate. The cavity itself was optimized to achieve both spatial uniformity over a rectangular exit which featured a pseudo-Lambertian emission angle, while the interior of the cavity was a box shape made of bare aluminum with a surface roughness of 3.4 m RMS. The system was modeled in LightTools, a non-sequential ray tracing simulation software, and the location of the heating elements, as well as interior cavity dimensions and surface roughness, were optimized to achieve a uniform power output across the exit slit while maintaining non-directional output over approximately 2 steradians. The output was simulated at the slit, where uniform power was the goal. The near field irradiance pattern, as well as the final optimized box design, are shown below in Figure 3.

3 LITMIS EXPERIMENTAL MEASUREMENT SETUP AND RESULTS

3.1 Deflectometry hardware, UUT, and source configuration

An infrared deflectometry system was configured such that all hardware was common, except the source, which was changed during experimental measurements. The Thermal-Eye 3500AS LWIR camera featured a ~1– 2 m variable focal length germanium lens, and its detector was

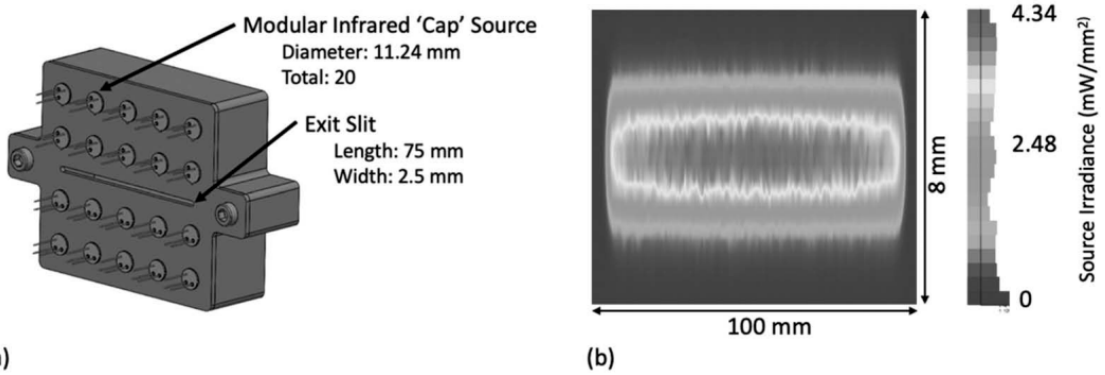

Figure 3. The final optimized LITMIS assembly was modeled in SolidWorks (a). 20 infrared emitters point inside a diffusing cavity which contains a single exit slit, machined from a thin aluminum plate. The optimized design was also modeled in LightTools, where the irradiance at the surface of the box was simulated to assure high uniformity across the exit slit (b).

a 160 × 120 microbolometer array with 320 × 240 super-resolution output. Exposure, gain, and level settings were adjusted to prevent output saturation and were held constant between all tests. A fixed optical mount was situated approximately one meter from the camera and allowed for repeatable UUT placement. To compare properties between source modalities, a scanning platform was utilized with a mounting interface to interchange LWIR sources. A motorized lead screw stage moved source assemblies in the vertical direction with an absolute positional accuracy of ±0.005 mm. For ease of comparison, sources shared both identical slit dimensions (75 mm × 2.5 mm) and radiant exitance planes. Figure 4 demonstrates the camera and source setup for the test system.

UUTs included a 2-inch diameter rough ground glass referred to as $Glass^{1500}$ and a bare aluminum flat referred to as Al_{Room}. UUTs were selected for measurement due to their diffuse nature, making thermal infrared deflectometry an ideal metrology method. When heated to 150°C, Al_{Room} flat is referred to as Al_{150}, and is done so as a challenge case because it generates variable thermal background noise, which typically degrades the SNR of a test. This is a common scenario, as several optics, such as solar collectors or even the DKIST primary mirror, will operate under thermal load; thus, the Al_{150} test case is highly relevant. The surface roughness of both optics was measured using a Zygo NewView 8300 Interference Microscope. The ground glass surface featured a surface roughness of 127.89 nm RMS while the bare aluminum surface roughness was 102.53 nm RMS over a small 834 × 834 µm square area over each optic.

The LWIR line source was implemented by running direct current (2.2 A, 2.1 W) across a thin 32 µm rectangular tungsten ribbon. Transient thermal noise from the wire, such as the local heating of air, was reduced by taking measurements only after the ribbon reached a thermal steady-state condition, which was achieved after approximately 20 minutes.

The LITMIS source was implemented by applying a (0.29 A, 7 W) load to a circuit consisting of 20 emitters. Pointed into the enclosure, the rectangular emitter array was operated by binary power cycling with a digitally controlled relay. Enclosure walls were machined from bare Al 6061-T6 and characterized to 3.4 µm RMS by a Zygo NewView 8300 Interference Microscope. Lastly, to minimize latent thermal radiation from the cavity interior, the LITMIS source was cooled to 0°C prior to each test. Figure 5 displays the integrating cavity after assembly.

3.2 Measurements and results for source geometry and temporal stability

Geometrical profile measurements were conducted by recording an image focused at each source with the LWIR camera. The camera software was adjusted so the maximum 8-bit signal count was a discrete value just below 255. Source profiles were captured and compared against

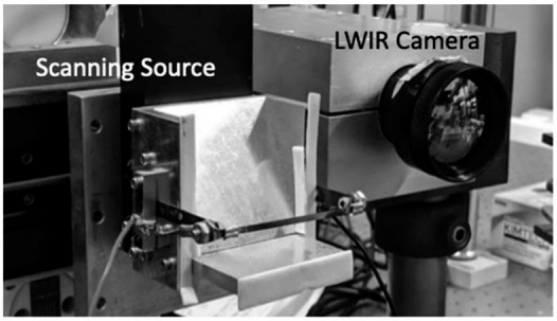

Figure 4. A traditional tungsten ribbon scanning source is mapped to Thermal-Eye 3500AS camera. As a requirement for deflectometry measurement, the camera is focused on the surface of the UUT. LWIR radiation leaves the source, of which, some rays are intercepted by the detector. For ground optics, higher SNR is required to precisely, or at all, determine the surface slope at a given mirror pixel. After UUT measurement with the ribbon, it is unmounted and replaced by the LITMIS source.

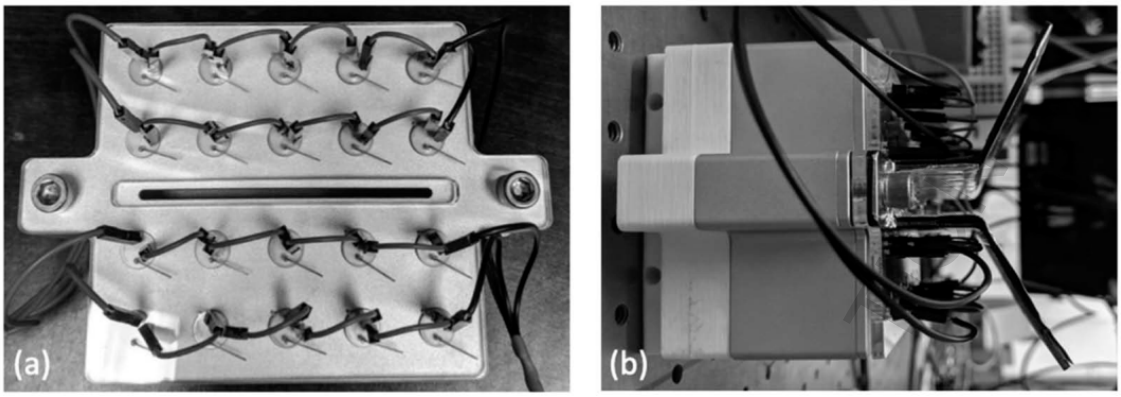

Figure 5. A frontal view of the assembled LITMIS architecture is shown in (a). Four parallel chains of elements are connected to operate as a single electrical circuit. While radiative thermal input is intended towards the interior of the box, excess thermal radiation is emitted by the heated copper body of each cap. Aluminum-covered shielding is mounted to the LITMIS façade to deflect it, as shown in (b). By design, LWIR radiation does not propagate directly from a heat source to the object of measurement. Rather, it is diffused by internal scattering and may only escape through a limited window. With this mechanism, input power can be readily scaled by simply adding more emitters within the cavity. In contrast, the available input power from a direct thermal source is limited by the area ofi ts profile geometry.

to an assumed ideal rectangular emission profile. As seen in Figure 6, the LITMIS source maintains a flatter signal power across the horizontal pixel band and drops off sharply at the edges.

To observe the temporal stability, a measurement was performed by focusing the camera on each source, which was turned on and recorded for 30 minutes, separately. Temporal measurement results illustrate the high stability and uniform slit emission

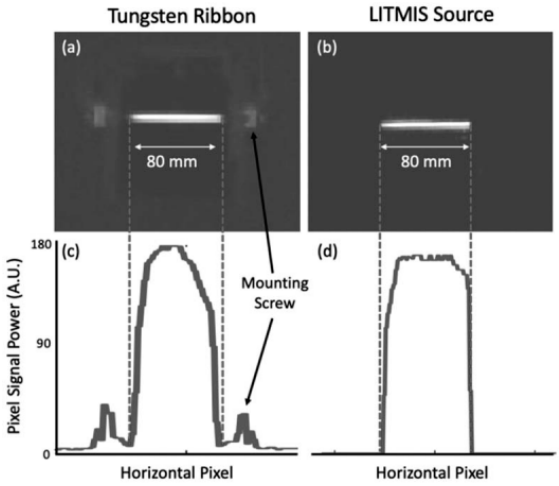

Figure 6. The images of the tungsten ribbon (a) as well as the LITMIS slit (b) sources were captured using Thermal-Eye 3500AS camera through-focused onto the source through a flat mirror. Observing the camera signal power histograms for the tungsten ribbon (c) and the LITMIS slit (d) sources, it is seen that the average power is similar, but the source profile geometries are quite different, where both should ideally form a flat top rectangular shape with roll-on and roll-off at the edges. This is due to the convolution of the rectangular source with the circular camera pupil.

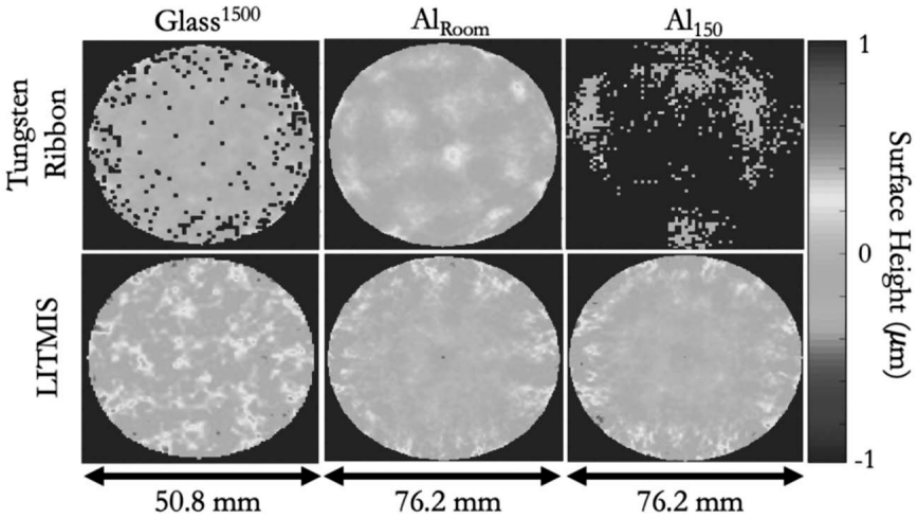

Figure 7. Using both a traditional tungsten ribbon source (top row) and the LITMIS source (bottom row), infrared deflectometry measurements were taken and the surface reconstructed for the Glass^{1500} optic (left column), the Al_{Room} optic (middle column), and the Al_{150} optic (right column). For all maps, Standard Zernike terms 1:37 were removed to observe the surface mid-to-high spatial frequency topology. In the Glass case, some points in the aperture could not be sampled due to insufficient SNR. In the Al_{150} case, a majority of the surface topology was unavailable due to competitive thermal noise. With greater immunity from thermal noise, the LITMIS source obtained sufficient slope data to reconstruct all three samples.

geometry of the LITMIS source. Stability was most pronounced in the signal peak-to-valley fluctuation comparison, which was measured as 11 signal counts for the tungsten ribbon source and 1.82 for the LITMIS source.

3.3 Measurements and results for UUT surface reconstruction and repeatability

To determine the comparative surface reconstruction repeatability, the Glass^{1500}, Al_{Room}, and Al_{150} optics were measured using both tungsten ribbon and LITMIS sources.

The reconstructed surface topology maps of all 3 UUT cases are shown in Figure 7. Both the LITMIS slit source and tungsten ribbon source were successfully used to test the Glass^{1500} and Al_{Room} optics. However, the standard deviation of the signal power across the five repeat measurements performed for every optic for each source was slightly larger for the tungsten ribbon as compared to the LITMIS source. Despite this, the LITMIS source was better able to reduce noise for all cases, which directly impacts the SNR of both test methods. Overall, the LITMIS source achieved a 25 times larger SNR for the Glass^{1500} and Al_{Room}. The Al_{150} sample could not be measured using the ribbon source due to high thermal noise generated by the UUT, while the LITMIS source provided sufficient slope data for surface reconstruction.

4 CONCLUSIONS

In infrared deflectometry, any uncertainty in the spatial and temporal behavior of a source directly negatively impacts the reconstruction accuracy and uncertainty. Additionally, time-varying, thermal background noise is common in most test environments and degrades the effectiveness of LWIR sources by decreasing the signal-to-noise ratio. We have instead created an integrating cavity source, which emits long-wave infrared light uniformly from a defined exit slit, which we call the LITMIS source. A demonstration infrared deflectometry system

using the new source successfully tested a ground glass sample and aluminum blank, as well as a previously unmeasurable aluminum blank under thermal load. In all cases, the source exhibited excellent repeatability and significantly improved the SNR of the test, as compared to testing using a traditional tungsten ribbon. The authors encourage readers to examine further detailed test results and analysis in the paper, "High-contrast thermal deflectometry using long-wave infrared time-modulated integrating cavity." (Graves et al., in prep.)

The scalability and flexibility of the new source architecture leave much to explore. Beyond simply engineering the source design to achieve high signal output power, temporal behavior may be exploited to reconstruct shapes of challenging optics. As temporal modulation adequately inoculates measurement from local thermal fluctuations in active workpieces, the creation of an on-machine deflectometry system also edges towards the realm of possibility. More excitingly, these building blocks may be applied towards a sinusoidally modulated infrared source, which may allow phase-shifting infrared deflectometry to become viable in optical metrology.

ACKNOWLEDGMENTS

The authors would like to acknowledge the II-VI Foundation Block-Gift Program for helping support general deflectometry research in the LOFT group, making this research possible. Also, this work was made possible in part by the Technology Research Initiative Fund Optics/ Imaging Program and the Korea Basic Science Institute Foundation.

REFERENCES

Aftab, M., Burge, J.H., Smith, G.A., Graves, L.R., Oh, C.J. and Kim, D.W. 2018. 'Chebyshev gradient polynomials for high resolution surface and wavefront reconstruction', 1074211(September 2018), p. 40. doi:10.1117/12.2320804.

Axetris AG 2014. 'IRS Frequently Asked Questions Rev.A', pp. 2–5.

Axetris AG 2019. 'Infrared Sources Brochure (English)', pp. 42–75. doi:10.1201/9780203750834-3

Dubin, M.B., Su, P. and Burge, J.H. 2009. 'Fizeau interferometer with spherical reference and CGH correction for measuring large convex aspheres', Optical Manufacturing and Testing VIII, 7426 (May), p. 74260S. doi:10.1117/12.829053.

Esfahani, S. and Covington, J.A. 2017. 'Low Cost Optical Electronic Nose for Biomedical Applications', Proceedings, 1(10), p. 589. doi:10.3390/proceedings1040589

Fang, F.Z., Zhang, X.D., Weckenmann, A., Zhang, G.X. and Evans, C. 2013. 'Manufacturing and measurement of freeform optics', CIRP Annals - Manufacturing Technology, CIRP, 62(2), pp. 823–846. doi:10.1016/j.cirp.2013.05.003.

Graves, L.R., Quach, H., Koshel, J.R., Oh, C.J., Kim, D.W. (in prep). 'High contrast thermal deflectometry using long-wave infrared time-modulated integrating cavity'.

Graves, L.R., Quach, H., Choi, H. and Kim, D.W. 2019. 'Infinite deflectometry enabling 2π-steradian measurement range', Optics Express, 27(5), p. 7602. doi:10.1364/oe.27.007602.

Hessler, T., Dubochet, O., Forster, M. and Merschdorf, M. 2004. 'Micro-machined, electrically modulated thermal infrared source with black body characteristic pyroelectric detectors', (November 2015).

Höfer, S., Burke, J. and Heizmann, M. 2016. 'Infrared deflectometry for the inspection of diffusely specular surfaces', Advanced Optical Technologies, 5(5–6), pp. 377–387. doi:10.1515/aot-2016-0051.

Kim, D.W., Su, T., Su, P., Oh, C., Graves, L. and Burge, J. 2015. 'Accurate and rapid IR metrology for the manufacture of freeform optics', SPIE Newsroom, pp. 9–11. doi:10.1117/2.1201506.006015.

Kim, D.W., Oh, C., Lowman, A., Smith, G.A., Aftab, M. and Burge, J.H. 2016. 'Manufacturing of super-polished large aspheric/freeform optics', Advances in Optical and Mechanical Technologies for Telescopes and Instrumentation II, 9912, p. 99120F. doi:10.1117/12.2232237.

Lowman, A.E., Yoo, H., Smith, G.A., Oh, C.J. and Dubin, M. 2018. 'Improvements in the scanning long-wave optical test system', 1074216(September 2018), p. 48. doi:10.1117/12.2321265.

Martin, H.M. et al. 2018. 'Manufacture of primary mirror segments for the Giant Magellan Telescope', (May), p. 30. doi:10.1117/12.2312935.

Oh, C.J. et al. 2016. 'Fabrication and testing of 4.2m off-axis aspheric primary mirror of Daniel K. Inouye Solar Telescope', 9912, p. 99120O. doi:10.1117/12.2229324.

Southwell, W.H. 1980. 'Wave-front estimation from wave-front slope measurements', Journal of the Optical Society of America, 70(8), p. 998. doi:10.1364/josa.70.000998.
Su, T., Park, W.H., Parks, R.E., Su, P. and Burge, J.H. 2011. 'Scanning Long-wave Optical Test System: a new ground optical surface slope test system', Optical Manufacturing and Testing IX, 8126(May), p. 81260E. doi:10.1117/12.892666.
Su, T., Wang, S., Parks, R.E., Su, P. and Burge, J.H. 2013. 'Measuring rough optical surfaces using scanning long-wave optical test system 1 Principle and implementation', Applied Optics, 52(29), p. 7117. doi:10.1364/ao.52.007117.
Verret, D.P. and Ramanathan, K.G. 1978. 'Total hemispherical emissivity of tungsten', Journal of the Optical Society of America, 68(9), p. 1167. doi:10.1364/JOSA.68.001167.
Wilson, D., Phair, J. and Lengden, M. 2019. 'Performance Analysis of a Novel Pyroelectric Device for Non-Dispersive Infra-Red CO_2 Detection', IEEE Sensors Journal, 1748(c), pp. 1–1. doi:10.1109/jsen.2019.2911737.